Chitosan / essential oils biocomposites for suppressing the growth of *Aspergillus parasiticus*

[1]Villegas-Rascón, R. E., [1]Plascencia-Jatomea, M., [1]Rosas-Burgos, E. C., [2]López-Franco, Y. L., [3]Tánori-Córdova, J. C., [4]López-Meneses, A. K and [1]*Cortez-Rocha, M. O.

[1]*Departamento de Investigación y Posgrado en Alimentos, Universidad de Sonora, Blvd. Luis Encinas y Rosales s/n. Col. Centro. Hermosillo, Sonora, C.P. 83000, México*

[2]*2Centro de Investigación en Alimentación y Desarrollo, A. C. Carretera Gustavo Enrique Astiazarán Rosas, No. 46. Col. La Victoria, CP. 83304*

[3]*Departamento de Investigación en Polímeros y Materiales, Universidad de Sonora, Blvd. Luis Encinas y Rosales s/n. Col. Centro. Hermosillo, Sonora, C.P. 83000, México*

[4]*Universidad Estatal de Sonora Unidad Hermosillo, Blvd. Rosales #189 Col. Centro, Hermosillo, Sonora, C.P. 83000, México*

Abstract

Cinnamon, thyme, and eucalyptus essential oils encapsulated in chitosan at different concentrations of 125, 250, 500, and 1000 ppm were synthesised by ionotropic gelation, and their efficacy was analysed against *Aspergillus parasiticus* and aflatoxin production. These nanoparticles were characterised by Fourier transform infrared spectroscopy (FTIR) and transmission electronic microscope (TEM). The diameter, Z potential, and morphology of the essential oils encapsulated in chitosan were significantly affected by the addition of the essential oils. Radial growth and spore germination were reduced during the first 24 h of incubation, and no effects were detected on aflatoxin production. The present work revealed that cinnamon and thyme essential oils encapsulated in chitosan could delay the first stage of *A. parasiticus* spore germination.

Introduction

Aspergillus is one of the three most important fungal genera in the spoilage of foodstuffs and production of various mycotoxins, with the other two genera being *Fusarium* and *Penicillium* (Degola *et al.,* 2015). *Aspergillus* produce the mycotoxin aflatoxins (AFB_1, AFB_2, AFG_1, and AFG_2), among which, AFB_1 is the most potent naturally occurring hepatocarcinogenic compound recognised as a Class 1 human carcinogenic agent by the International Agency for Research in Cancer (IARC). Thus, AFB_1 contamination may cause significant economic losses as well as impose threats to animal and human health (Williams *et al.,* 2004). Synthetic chemical fungicides are the main compounds used to prevent and control fungal contamination. However, because of the disadvantages they present for the environment and public health, users have attempted to replace their use with compounds of natural origin, such as essential oils (EO) (Sotelo-Boyás *et al.,* 2017a). EO are natural lipophilic, volatile, and complex compounds produced by plants as secondary metabolites, characterised by a strong aroma and extensive biological activity (Russo *et al.,* 2012; Soliman *et al.,* 2013).

Furthermore, many EO also possess strong antifungal properties, not only by direct contact but also in their vapor phase. Thus, their application in the pre- or post-harvest stage of plant products may be considered an alternative treatment to the use of synthetic fungicides. However, EO bioactivity is often limited because their volatile compounds can easily degrade due to the action of heat, pressure, light, and oxygen. Therefore, it is important to use techniques that help maintain the physical stability of EO, such as micro- and nano-encapsulation (Mohammadi *et al.,* 2015). In micro- and nano-particles, components of EO are encapsulated or embedded in polymer matrices, and one of the materials that has proven effective for the encapsulation of these active compounds is chitosan (Prakash *et al.,* 2018; Alavi and Nokhodchi, 2020). Chitosan exhibits a dual modes of action, on the pathogen and on the plant, as it reduces the growth of decay-causing fungi and foodborne pathogens, and induces resistance responses in the plant tissues (Romanazzi *et al.,* 2017). Chitosan is known for its antimicrobial activity against a wide range of microorganisms. Three mechanisms have been proposed to explain its activity. One of the most acceptable antimicrobial mechanism is due to the

*Corresponding author.
Email: mario.cortez@unison.mx

presence of positively charged groups in the polymer backbone and their ionic interactions with microbial cell wall constituents (Goy *et al.,* 2016). The second mechanism proposes that chitosan acts as a chelator of essential micronutrients such as Ca^{2+} and Mg^{2+} that may induce malformations of microbial cells (Xing *et al.,* 2015). In addition, the emergence of silver chitosan nanocomposites (AgNP) has demonstrated effective antimicrobial effects resulting from the large surface area-to-volume ratio and from the high-aspect ratio of AgNP as compared to their bulk (Alavi and Rai, 2019). Depending on the microbial type, there are several inter-actions of released Ag^+ ions with the cell wall and mem-brane components, and these ions can bind to thiol (R-SH) groups of membrane proteins and inhibit the respiratory function of the microorganisms (Alavi and Karimi, 2019). The third mechanism establishes that low-molecular weight chitosan is capable of penetrat-ing the cell's nucleus, thus interacting with the DNA, interfering with the synthesis of messenger RNA, affecting the synthesis of proteins, and inhibiting the action of various enzymes (Rodríguez *et al.,* 2005).

Moreover, several authors have evaluated the antifungal and antibacterial activity of different EO / chitosan treatments. Mohammadi *et al.* (2015) evaluat-ed the effect of chitosan nanoparticles loaded with cinnamon EO on cucumbers infected with *Phytophtora drechsleri*. They found that cinnamon EO encapsulated in chitosan exhibited higher performance than EO and chitosan individually. Other studies have focused on the synergistic effect of the antimicrobial activity of chitosan and EO on diverse microorganisms (Soliman *et al.,* 2013). Nonetheless, to date, there are, to our knowledge, no records on the antifungal effect of chitosan nanoparticles with the EO of cinnamon, thyme, and eucalyptus on *Aspergillus parasiticus*; how-ever, they have demonstrated excellent results in other fungal species (Liu *et al.,* 2017). Therefore, the objec-tive of the present work was to synthesise, characterise, and evaluate the antifungal properties of chitosan nano-particles with the EO of thyme, cinnamon, and eucalyp-tus against *A. parasiticus* and aflatoxin production.

Materials and methods

Raw materials
Commercial medium-molecular weight (153 kDa) chitosan (CS) of 67% deacetylation grade (cat. 448877), sodium tripolyphosphate TPP (cat. 238503), cinnamon (CEO) (*Cinnamomum zeylanicum,* cat. w-22921-0), and thyme (TEO) (*Thymus capitatus*, cat. w-28281-2) essential oils were acquired from Sigma Aldrich® (St. Louis, MO, USA), and Tween 80 from Faga Lab. (Culiacán, Sinaloa, México). Eucalyptus

(*Eucalyptus camaldulensis*) essential oil (EEO) was obtained by hydrodistillation from leaves collected in Hermosillo, Sonora, México.

Microbial growth conditions
Aspergillus parasiticus (ATCC 16992) was activated at $27 \pm 2°C$ in potato dextrose agar medium (PDA) for 7 d in the dark until sporulation. The spores were harvested in 1% (v/v) Tween 80 into a flask and stirred on a magnetic stirred hot plate (Barnstead thermoline cimerac SP131015, USA) for 10 min. The spore suspension was adjusted to $1 \times 10^5/mL$ with a Neubauer chamber, and was utilised to monitor the effects of nanomaterials on fungal growth and AFB_1 production.

Eucalyptus essential oil (EEO) extraction
The collected leaves were washed using tap water, dried at room temperature (25°C) for 7 d, and cut into thin pieces. For EEO extraction, leaf sample (100 g) was placed in a three-inlet ball flask with 300 mL of distilled water and mounted in hydrodistillation extraction equipment with a trap type Clevenger (IMPARLAB, México), a heating jacket (CIVEQ, México), and a cooling system (LAUDA Alpha 8, USA). The distillation process was carried out for 4 h, as reported by Said *et al.* (2016). The extracted EO was recovered in a 1.5 mL dark-brown glass vial and stored at 4°C. The extraction yield was calculated as the ratio of EO weight to the leaf weight.

Chemical characterisation of essential oils
The chemical composition of the EO was deter-mined by using a gas chromatograph GC-7890B, according to Said *et al.* (2016). The constituents of each EO were identified by comparing linear retention rates based on a mixture of *n*-alkanes at spectral retention times obtained with the NIST 98 database (National Institute of Standard and Technology, USA).

Determination of inhibitory concentrations 50 (IC_{50}) of EO's
To determine the IC_{50} of each EO, a radial growth test was performed, as described by López-Me-neses *et al.* (2018). For this, four concentrations of each EO were prepared: 125, 250, 500, and 1,000 ppm. These were incorporated in an emulsion with Tween 80 (1%) in a Falcon tube with Czapek agar, stirred in a vortex, and poured into 25 mL Petri dishes. Three controls were prepared: Czapek, Tween (Czapek agar + 1% Tween 80), and Terravax® (a commercial fungicide, captan 20% + carboxin 20%, 2.5 g/L) as positive control. Finally, 6-mm diameter wells were drilled using the top of a sterile pipette in the centre of each

plate for inoculation. A suspension of 1×10^6 spores/mL of *A. parasiticus* was inoculated by spot deposition onto individual Petri dishes. The colony radial-extension growth in each treatment was measured daily and compared with those from controls. The percentage of radial inhibition was calculated using Eq. 1:

$$\text{Radial inhibition (\%)} = \left[1 - \left(\frac{Xi}{Xc}\right)\right] \times 100$$

(Eq.1)

where, Xc = average radius of the colony in control medium, and Xi = colony radius in each treatment. Once the percentages of radial-growth inhibition by the EO were obtained, the minimum inhibitory concentration was calculated by employing NCSS software (version 2001, NCSS Statistical Software, USA).

Synthesis of CS-EO nanoparticles

Chitosan nanoparticles are usually prepared using various techniques such as cross-linking anions, precipitation, coacervation, and ionotropic gelation, among others. In the present work, ionotropic gelation was employed due to its mild process that avoids the use of organic compounds and high temperatures (Dananjaya *et al.*, 2017). The synthesis of EO encapsulated in chitosan involves a two-step process as follows: preparation of an oil-in-water emulsion and ionotropic gelation (Keawchaoon and Yoksan, 2011). The first step was to prepare a chitosan solution (0.2%, w/v) in acetic acid (1%, v/v), which was stirred using a magnetic bar at 50°C for 2 d. Then, this was filtered through 1.6-μm filter paper and the pH was adjusted to 4.6 using a 0.1 N sodium hydroxide (NaOH) solution. Later, Tween 80 (0.225 g) was added as surfactant to the chitosan solution and stirred magnetically at 50°C for 2 h. Subsequently, 0.02 g of each EO was added. Each emulsion was left under magnetic stirring at 25°C for 1 h to obtain a homogeneous mixture of Chitosan-Tween 80-Essential Oil (CS-Tw80-EO).

In the second step, a solution of TPP, 0.02% (w/v), was prepared. This was left to drip (3 mL) into the CS-Tw80-EO mixture with constant magnetic stirring at a flow rate of 0.3 mL/min by means of a peristaltic pump (Bio-Rad Laboratories, CA, USA). Then, it was magnetically stirred for 15 min, resulting in the EO encapsulated in chitosan (CS-EO), CS with CEO (CS-CEO), and CS with TEO (CS-TEO) (Feyzioglu and Tornuk, 2016). Subsequently, it was dialysed with a 12-KDa membrane (Sigma-Aldrich) to eliminate the materials remaining from the synthesis process. Two washes with 10% methanol (v/v) every 12 h were performed using constant magnetic stirring; subsequently, two more washes were carried out every 12 h using deionised water.

Physicochemical characterisation of the CS-EO
Fourier transform infrared spectroscopy (FT-IR)

The interaction between the chitosan functional groups with each EO was analysed by using FT-IR spectra. Perkin-Elmer FT-IR Spectrum GX equipment (Waltham, MA, USA) with an average of 16 scans within a spectral range of 4000 - 400 cm^{-1} was employed (Keawchaoon and Yoksan, 2011; Luque-Alcaraz *et al.*, 2016).

Transmission electron microscopy (TEM)

The morphology of the CS-EO nanoparticles was analysed in a JEOL transmission electronic microscope (TEM) with 200-kV operating voltage and field emission filament (JEM 2010F JEOL, USA), as described by Keawchaoon and Yoksan (2011). For this, one drop of each EO encapsulated in chitosan was allowed to dry at 25°C on a copper grid coated with a 400-mesh carbon film (FCF400-Cu). Afterward, 10 μL of 2% phosphotungstic acid was added to each sample and left to act for 5 min, while removing the excess. Finally, the samples were placed in a vacuum chamber for 18 h and observations were made in the 200-nm field.

Particle size and Zeta potential (ZP)

The Zeta potential (ZP) is the electric potential in the double interfacial layer, which is the place where the diffuse and the Stern layers are bonded. Its value is associated with the stability of the colloidal dispersions, indicating the repulsion degree among adjacent particles charged in a dispersion. The particle size and Zeta potential of EO encapsulated in chitosan were determined by dynamic light scattering (DLS), as in Luque-Alcaraz *et al.* (2016), utilising Möbius equipment (Wyatt Technology Corporation, USA). Each nanoparticle was diluted in MilliQ water (1:100, v/v) to avoid aggregation and placed in an electromagnetic capillary cell to determine the Zeta potential. Each determination was carried out in triplicate.

Encapsulation efficiency and loading capacity

The content of each EO loaded in the chitosan was determined by UV-vis spectrophotometry (Keawchaoon and Yoksan, 2011). For this, 10 mg of each EO encapsulated in chitosan was added to 4 mL of HCl (2 M) to release the encapsulated EO from the chitosan, and boiled at 95°C for 30 min. After cooling, 2 mL of ethanol was added as dispersion media for the EO, and centrifuged (Hermle model Z 216 MK Labortechnik, Germany) at 9,000 rpm for 5 min at 25°C. Supernatant was collected and

the content of each EO was measured using a UV-vis spectrophotometer (BioMate 3S, Thermo Fisher Scientific, USA) at 300 nm. The amount of EO was calculated using a calibration curve of each free EO in ethanol ($R^2 = 0.999$). In addition, a blank sample was run for a sample of chitosan, which was processed in a similar way. Each batch of samples was measured in triplicate. The encapsulation efficiency (EE) and loading capacity (LC) of each EO were calculated using Eq. 2 and Eq. 3:

$$EE\ (\%) = \frac{Total\ amount\ of\ loaded\ \text{EO}}{Initial\ amount\ of\ \text{EO}} \times 100$$

(Eq. 2)

$$LC\ (\%)\ \frac{Total\ amount\ of\ loaded\ \text{EO}}{Weight\ of\ CS-EO\ after\ freeze\ drying} \times 100$$

(Eq. 3)

Antifungal assays
Radial growth

To evaluate the antifungal activity of *Aspergillus parasiticus* radial growth in the presence of EO encapsulated in chitosan, we employed the point deposition method, identical to that described for IC_{50} determination. Czapek agar was prepared and deposited in 25-mL Petri dishes and amended with each type of nanoparticle in the IC_{50} determined for each EO. Also, three controls were prepared: Czapek control, CS control (Czapek + 0.2% chitosan solution [7:3], and TPP control (plates with Czapek medium and 0.02% TPP). A 6-mm hole in the centre of each Petri dish was drilled and an inoculum of 1×10^5 spores/mL was deposited, and plates incubated under the conditions previously described. Radial growth of the colony was measured with a ruler every 24 h until the colony in the Czapek control plate totally covered the surface.

Germination and morphometry of spores

Spore germination is an indicator of fungal adaptation to adverse factors in the medium; thus, the effects of EO encapsulated in chitosan exerted on *A. parasiticus* spore germination was evaluated according to Cota-Arriola *et al.* (2013) with modifications. For this, 12-well microplates (Costar, Corning Inc, USA) were employed, adding 1 mL of liquid Czapek medium (pH = 5.6) to the nanoparticles (in the IC_{50} of each EO) in each well, along with the controls used in the radial growth. Each treatment was inoculated with 1×10^6 spores/mL and incubated using a 12-h light/dark cycle in a precision, low temperature illuminated incubator (Precision model 818, USA) at $27 \pm 2°C$. Every 6 h, a sample of each treatment and

control was taken and placed on a coverslip. Then, with an optical microscope (Olympus CX-311, Japan), 100 spores were counted at random, determining the number of germinated and non-germinated spores. The percentage of inhibition was calculated using Eq. 4:

$$\text{Germinated spores inhibition (\%)} = \left(\frac{\%Sc - \%St}{\%Sc}\right) \times 100$$

(Eq. 4)

where, *%Sc* = percentage of germinated spores in the control, and *%St* = percentage of spores germinated in each treatment.

Spores from the germination test were also utilised to measure the average diameter and to determine possible morphometric changes. Image analysis was carried out by using an Image-Pro Plus software version 6.3 (Media Cybernetics Inc., USA) in an optical microscope (Olympus CX31, Japan) connected to an Infinity 1 camera, employing a 40× objective.

Septate count

The count of septate in the hyphae of the fungus was carried out by fluorescence microscopy, as described by Cota-Arriola *et al.* (2013). Twelve-well microplates were used and 1.0 mL of Czapek liquid medium (pH = 5.6) was added to each well with each of the nanoparticles in the IC_{50} of each EO. Each well was inoculated with 1×10^6 spores/mL of *A. parasiticus* and the microplates were incubated for 12 h at $27 \pm 2°C$ in darkness. A fresh smear from each of these inocula was taken and added to 1 - 2 drops of calcofluor white dye (10 µ g/mL). Images of the septate formation were taken in an epifluorescence microscope (Leica DM2500, USA), with a blue-violet filter at an emission and excitation wavelength of 330 - 380 and > 420 nm, respectively. Each experiment was performed in triplicate.

Anti-aflatoxigenic assay

The effectiveness of the EO encapsulated in chitosan, TPP, and EO alone against aflatoxin B_1 production was evaluated as follows: samples of 50 g of healthy maize grain were placed in 125-mL flasks, the humidity was adjusted to 25%, and these were sterilised for 2 d in autoclave (AESA model CV 300, Mexico) for 15 min at 121°C. The sterilised grains were treated separately with 10 mL of the nanoparticles in the IC_{50} of each EO. The following controls were prepared: maize (without inoculum or treatment), water, CS, TPP, CEO, and TEO. Each flask was inoculated with 1×10^5 spores/mL of *A. parasiticus*

and incubated in the dark for 16 d at 27 ± 2°C. Three repetitions were carried out for each treatment. For aflatoxin extraction and quantification, immunoaffinity columns from VICAM Aflatest kits (Waters Corporation, USA) were used, following the manufacturer's specifications for fluorometer quantification.

Statistical analysis

Data were expressed as means ± standard deviations of three replicates ($n = 3$). Means were then subjected to an analysis of variance (ANOVA). The significant difference between treatments was determined using the Tukey's multiple range test ($p \leq 0.05$), with the JMP statistical software program.

Results and discussion

Extraction of eucalyptus essential oil and chemical characterization of all oils

Eucalyptus essential oil (EEO) presented yellow coloration and the characteristic aroma of this plant. The EEO yield was $0.8 \pm 0.1\%$ in dry basis, which is lower than those reported by Mubarak *et al.* (2015) and Elaissi *et al.* (2010), at 1.4 and 1.3%, respectively, by hydrodistillation. Although it is the same plant species, the variability in the EO yield is attributed to several factors, such as the soil, the age of the tree, climate, and time of harvest (Mubarak *et al.,* 2015).

The chemical composition of EEO was determined, whereas the composition of cinnamon and thyme EO had already been determined (Villegas-Rascón *et al.,* 2018). Carvacrol was the major compound (46.2%) in *Thymus capitatus*, eugenol (70%) in *Cinnamomum zeylanicum*, and 3,3,3-trimethyl-1,3,5-cycloheptatriene (22.9%) in *Eucalyptus camaldulensis*. It was reported that in cinnamon EO, the major compound found was eugenol (Nabavi *et al.,* 2015), in thyme EO, it was carvacrol (Russo *et al.,* 2012; Jemaa *et al.,* 2018), while in eucalyptus EO, they were γ-terpinene and 1,8-cineol (Mubarak *et al.,* 2015). In the present work, 3,3,3-trimethyl-1,3,5-cycloheptatriene was the main component. This variability of major compounds in EO, even within the same species, could be due to various factors that affect the plant´s development and processing. Geographical origin, climatic conditions, soil, biotic and technological factors, cultivation techniques, types of harvesting processes, and the storage conditions of raw material as well as processing technologies are some examples of such factors (Russo *et al.,* 2012).

Physicochemical characterisation of CS-EO nanoparticles

The CS-TPP control nanoparticles (without incorporated oil) had an average diameter of 478.9 nm, which was significantly different ($p < 0.05$) from those with EO incorporated (29.3 and 19.7 nm for CS-CEO and CS-TEO, respectively). Other authors have also encapsulated EO in chitosan, obtaining different particle sizes. Hosseini *et al.* (2013) prepared nanoparticles of chitosan with oregano EO, obtaining an average diameter of 282 nm for those with only chitosan and 310 - 402 nm for chitosan-EO nanoparticles. Also, Kalagatur *et al.* (2018) synthesised spherical chitosan nanoparticles with *Cymbopogon martinii* EO with a Zeta potential of 39.3 - 37.2 mV, whose size ranged from 455 - 480 nm, which is similar to our control. In addition, Sotelo-Boyás *et al.* (2017b) produced chitosan nanoparticles and nanocapsules with lime EO with an average size of 6.1 nm. In this respect, various factors could affect the size of chitosan nanoparticles, such as molecular weight, degree of deacetylation, concentration of chitosan, pH, and the ionic strength of the medium-in-suspension, as well as the method used (Mohammadi *et al.,* 2015; Sotelo-Boyás *et al.,* 2017b). On the other hand, no significant difference was found between the Zeta potential of CS-TPP and EO encapsulated in chitosan (+24.3, +22.9, and +22.7, respectively). Likewise, both nanoparticles presented positive charges, which is indicative of their physical stability due to the electrostatic repulsion between particles that remains (Luque-Alcaraz *et al.,* 2016).

The morphology of the nanoparticles was analysed by TEM and their micrographs are shown in Figure 1. The nanoparticles CS-TPP (a) had a spherical shape, and two main sizes were observed (ø = 16 - 23 and 54 - 84 nm). This finding is in agreement with a study of Dananjaya *et al.* (2017), who prepared chitosan nanoparticles and chitosan silver nanocomposites. They found that sizes obtained from DLS analysis were much larger than those observed by TEM. Similar results were reported by Luque-Alcaraz *et al.* (2016) in *Schinus molle* EO in chitosan nanoparticles and bionanocomposites. The particle sizes were not consistent with those previously mentioned because the hydrodynamic diameter is measured when using dynamic light scattering, which indicates the bimodal distribution for the new particles. Particle size measured by SEM differed from those measured by DLS; this could be due to the swelling capacity of the chitosan in solution with TPP, while those for SEM analysis were dry-prepared. With the incorporation of the EO, changes in
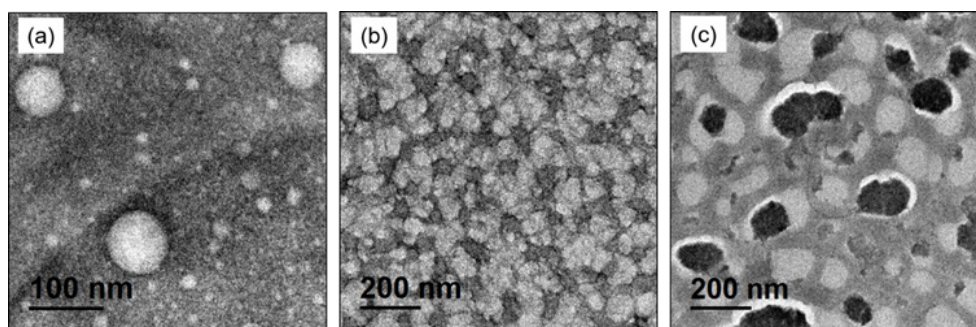
Figure 1. TEM micrographs of nanoparticles: a) CS-TPP (Control); b) CS-CEO; and c) CS-TEO.
CS = chitosan; TPP = Tripolyphosphate; CEO = Cinnamon EO; and TEO = Thymus EO.

the particle shape and dispersion were observed, probably due to the ordering of the phenolic compounds present in the EO and in the CS-TPP matrix. CS-CEO and CS-TEO nanoparticles exhibited irregularity in their morphology and a tendency toward aggregation. The morphological changes were more marked with CS-TEO, where particles with a tendency to oblong and non-uniform shapes were observed, with as greater contrast of sizes (higher than 75 nm).

The chemical composition of the nanoparticles was elucidated by FT-IR (Figure 2). In CS-TPP nanoparticles, intense bands were exhibited at 1569 (amide II), 1410 (CH flexion), 1040 (COC flexion), 651 (NH flexion out of plane), and 617 cm^{-1} (pyranose ring), and with less intensity in the region of 2987 and 2925 (CH stretch), which are characteristic of chitosan (Keawchaoon and Yoksan, 2011; Woranuch and Yoksan, 2013). The particles of cinnamon EO encapsulated in chitosan revealing an increase in the intensity of the bands were found in the regions 2920 and 2857 cm^{-1} (stretch of CH), which was probably due to the presence of CEO (Hosseini *et al.,* 2013). Similarly, bands were observed at 3394 (OH), 1735 (stretch C = O), 1572 (amide II), 1410 (CH flexion), 1092 (COC flexion), and 648 cm^{-1} (NH flexion out of plane) (Keawchaoon and Yoksan, 2011; Woranuch and Yoksan, 2013).

Additionally, CS-TEO nanoparticles exhibited bands very similar to those of CS-CEO, but with more intense peaks at 2925 and 2862 cm^{-1}. Both the CS-CEO and the CS-TEO exhibited wider and more intense bands between 3394 and 3432 cm^{-1} than those of CS-TPP. This is probably because of an increase in aromatic CH bonds (between 3000 and 3100 cm^{-1}), CH alkenes (between 3020 and 3018 cm^{-1}), and OH groups, which were present in the main active phenolic compounds of both EO.

Encapsulation efficiency (EE) and loading capacity (LC)

The percentage of EE and LC of TEO and CEO encapsulated in chitosan were low: 2 and 5%,
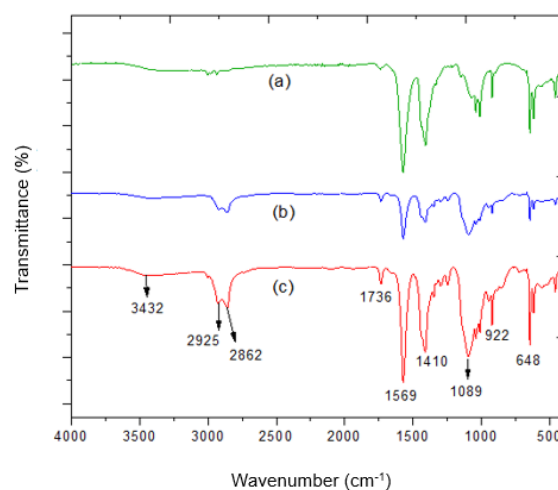

Figure 2. FT-IR spectra of nanoparticles: (a) CS-TPP (control); (b) CS-CEO; and (c) CS-TEO. CS = chitosan; TPP = Tripolyphosphate; CEO = Cinnamon EO; and TEO = Thymus EO.

and 4.8 and 8%, respectively. Our data are in agreement with previous studies involving the encapsulation of bioactive compounds by using the ionotropic gelation of chitosan cross-linked with TPP. Mohammadi *et al.* (2015) found that the EE and LC of CEO loaded in chitosan ranged from 1.99 - 16.9 and 3.1 - 3.78%, respectively. In addition, in the study of Hosseini *et al*. (2013), the LC and EE in encapsulated oregano EO (OEO) nanoparticles ranged from 5.45 - 24.7 and 1.32 - 2.12%, respectively. They mentioned that the LC increased as a function of the initial content of OEO, and the EE tended to decrease, a parameter which was not evaluated in our work.

Antifungal assays
Radial growth

The effects of EO on the radial growth inhibition is presented in Table 1. Statistical analyses showed that there was significant difference between the EO and concentrations evaluated ($p < 0.05$). Total inhibition of *A. parasiticus* radial growth was observed since the first 24 h of incubation in the

Table 1. Radial growth inhibition of *Aspergillus parasiticus* in the presence of essential oils in Czapek media incubated at 27°C.

Essential oil (ppm)	Incubation time (h)					
	24	48	72	96	120	144
C_{Cz}	0^d	0^g	0^i	0^i	0^h	0^k
Cinnamon						
125	100.0 ± 0.0^a	56.0 ± 7.4^{cd}	43.9 ± 2.6^{ef}	43.0 ± 1.9^e	34.4 ± 1.2^e	26.5 ± 1.3^{gh}
250	100.0 ± 0.0^a	74.3 ± 4.7^b	66.7 ± 2.6^c	64.5 ± 0.0^c	63.2 ± 1.2^{cd}	56.8 ± 2.3^e
500	100.0 ± 0.0^a	94.8 ± 4.5^a	86.4 ± 4.5^b	82.8 ± 1.9^b	80.8 ± 2.2^b	76.5 ± 1.3^c
1000	100.0 ± 0.0^a	100.0 ± 0.0^a	100.0 ± 0.0^a	100.0 ± 0.0^a	100.0 ± 0.0^a	100.0 ± 0.0^a
Thyme						
125	45.0 ± 18.0^{bc}	41.0 ± 2.3^{ef}	36.4 ± 4.5^f	37.6 ± 1.9^f	39.2 ± 1.2^e	29.5 ± 2.3^g
250	100.0 ± 0.0^a	59.0 ± 2.3^c	56.1 ± 2.6^d	57.0 ± 1.9^d	57.6 ± 0.8^d	50.0 ± 0.0^f
500	100.0 ± 0.0^a	76.6 ± 9.1^d	71.2 ± 2.6^c	68.8 ± 1.9^c	65.6 ± 3.0^c	61.4 ± 2.3^d
1000	100.0 ± 0.0^a	97.2 ± 4.8^a	87.9 ± 2.6^b	81.7 ± 1.9^b	83.2 ± 4.4^b	82.6 ± 2.6^b
Eucalyptus						
125	30.0 ± 8.7^c	30.7 ± 6.7^f	16.7 ± 2.6^h	19.4 ± 3.2^h	16.8 ± 0.2^g	6.8 ± 2.3^j
250	45.0 ± 18.0^{bc}	33.3 ± 2.5^f	21.2 ± 5.2^{gh}	21.5 ± 1.9^{gh}	18.4 ± 1.1^{fg}	8.3 ± 1.3^j
500	68.3 ± 16.1^b	43.4 ± 6.0^{def}	25.8 ± 2.6^g	25.8 ± 0.0^g	24.0 ± 2.1^f	13.6 ± 0.0^i
1000	100.0 ± 0.0^a	53.7 ± 3.6^{cde}	50.0 ± 0.0^{de}	38.7 ± 3.2^{ef}	36.0 ± 3.7^e	25.0 ± 0.0^h

Data are means ± standard deviation of triplicates (n = 3). Means in the same column with different letters are significantly different ($p \leq 0.05$). C_{Cz} = Control Czapek.

presence of the CEO followed by an inhibition of 82.6% produced with TEO after 144 h. Eucalyptus EO possessed a moderate capacity to reduce the growth, being less efficacious as compared with CEO and TEO. The concentrations of bioactive components in the EO and their chemical structure are responsible for their antifungal activity on mycelial growth and spore germination by affecting the cellular metabolism of the pathogens (Woranuch and Yoksan, 2013). Eugenol (4-allyl-2-methoxy phenol) was detected in high amounts (70%), caryophyllene (4.5%) in CEO, carvacrol (2-methyl-5-(1-methyethyl)-phenol, 46.2%), thymol (13.6%), O-cymene (12%), and β-pinene (6%) in TEO (Villegas-Rascón *et al,* 2018). Carvacrol, eugenol, and thymol contain high amounts of phenolic compounds in their chemical structure that allow them to exhibit strongest properties against fungal pathogens (Lambert *et al.,* 2001). Eugenol biological activity is related to the chemical structure of their components and their interaction along with the concentration in which they are present (Woranuch and Yoksan, 2013). Eugenol was detected in high amounts (70%) in CEO, and it is recognised for its antimicrobial activity, causing a disturbance in the cytoplasmic membrane, disrupting the proton motive force (PMF), electron flow, active transport, and coagulation of the cell contents. In addition, Pillai and Ramaswamy (2012) revealed that *A. parasiticus* growth was

completely inhibited by eugenol at 150 ppm. Juglal *et al*. (2002) also demonstrated the efficacy of clove EO to inhibit growth of *A. parasiticus* and *Fusarium moniliforme*. They found that this oil at 0.5 and 2.0 µL/mL completely inhibited the production of fumonisin B_1 and reduced the aflatoxins by 78%.

Determination of minimum inhibitory concentrations 50 (IC$_{50}$) of the EO

The calculated minimum inhibitory concentration (IC$_{50}$) for EEO was considerably higher than those from CEO and TEO (817.9, 118.0, and 178.3, respectively). Significant differences were found ($p <$ 0.05) between EO and the applied concentrations. CEO generated the greatest and most prolonged inhibitory effect in *A. parasiticus*, completely inhibiting its mycelial growth at 1,000 ppm until 144 h of incubation, followed by TEO (82.6% inhibition). In agreement with these results, we decided to prepare only nanoparticles with the CEO and TEO.

Spore germination and morphometric parameters

Spore germination comprises the first step of the fungal colonisation of substrates (Kocevski *et al.,* 2013). Table 2 presents the results of spore germination inhibition. Significant differences among treatments were found ($p <$ 0.05). Chitosan control caused 97% inhibition at 24 h of incubation. Nanoparticles of CS-TEO inhibited by 24.5% within the first 12 h,

Table 3. Diameter of spores (μm) of *Aspergillus parasiticus* exposed to nanoparticles of chitosan and essential oils (EO) at different incubation times at 27°C.

Treatment	Incubation time (h)			
	6	12	18	24
Cz	6.2 ± 0.0[a]	6.8 ± 0.1[a]	6.8 ± 0.0[ab]	6.9 ± 0.1[ab]
CS + Cz	5.4 ± 0.1[b]	5.4 ± 0.9[b]	5.4 ± 0.4[d]	5.4 ± 1.4[c]
TPP + Cz	5.9 ± 0.1[ab]	7.7 ± 0.6[ab]	6.5 ± 1.3[bc]	6.0 ± 3.3[abc]
CEO + Cz	6.0 ± 0.0[a]	6.7 ± 1.0[a]	7.0 ± 0.8[a]	5.2 ± 0.5[abc]
TEO + Cz	6.0 ± 0.0[a]	5.8 ± 2.1[a]	6.2 ± 0.4[c]	6.7 ± 0.8[bc]
Np CS-CEO + Cz	5.9 ± 0.0[ab]	6.9 ± 0.8[a]	6.9 ± 0.7[ab]	6.0 ± 0.7[a]
Np CS-TEO + Cz	6.0 ± 0.0[a]	6.6 ± 1.5[a]	7.0 ± 1.6[a]	7.1 ± 1.3[a]

Data are means ± standard deviation of triplicates (*n* = 3). Means in the same column with different letters are significantly different (*p* ≤ 0.05). CS = chitosan; TPP = Tripolyphosphate; CEO = Cinnamon EO; TEO = Thymus EO; and Cz = Czapek.

whereas those of CS-CEO maintained inhibition for 24 h. There was no statistical difference (*p* > 0.05) in spore diameters among the nanoparticles prepared with EO (Table 3). These demonstrated the same diameter in all of the treatments with respect to the control (from 6.0 - 7.1 μm). Our results suggest that synergism between chitosan and EO did not exist. We think that this was due to the proportion of Tween 80 used for nanoparticles preparation (78.4%) as compared to EO (13.9%) and for chitosan (6.97%), thus affecting their activity. In addition, interactions of the hydroxyl groups from phenolic compounds in the EO and in the chitosan amino groups were drastically reduced. This could probably be due to the interactions of chitosan with the aromatic, alkenes, and OH groups present in the major phenolic compounds of both EO.

Septate count

The cells of filamentous fungi grow as tubular structures called hyphae, which can be septated or not (coenocytic). Septate hyphae are partitioned into compartments separated by cross walls at more or less regular intervals. The septa of ascomycetous hyphae are not impenetrable barriers across hyphae because they generally possess a central pore that allows cytoplasm, organelles, and nuclei to pass through. Septum formation is an indicator of a rather close correlation between mitosis and septum construction (cell cycle and cell-wall biosynthesis) (Mouriño-Pérez, 2013). The precision with which the apical compartment of leading hyphae is delimited by septation suggests that septum initiation is a well-regulated event. In the present work, it was observed that there was presence of septate and

Table 2. Spore germination inhibition (%) of *Aspergillus parasiticus* exposed to nanoparticles of chitosan and essential oils (EO) at different incubation times at 27°C.

Treatment	Incubation time (h)			
	6	12	18	24
Cz	0[c]	0[d]	0[d]	0[e]
CS + Cz	100.0 ± 0.0[a]	100.0 ± 0.0[a]	96.5 ± 1.8[a]	97.0 ± 4.3[a]
TPP + Cz	52.8 ± 8.6[b]	1.5 ± 2.1[d]	0.0 ± 0.0[d]	17.1 ± 4.7[de]
CEO + Cz	100.0 ± 0.0[a]	58.3 ± 1.7[b]	18.9 ± 6.9[c]	72.3 ± 19.0[bc]
TEO + Cz	89.6 ± 1.9[a]	41.7 ± 1.7[bc]	58.8 ± 1.0[b]	87.1 ± 1.1[b]
Np CS-CEO + Cz	44.7 ± 21.6[b]	14.5 ± 8.4[d]	18.8 ± 6.3[c]	22.4 ± 1.6[d]
Np CS-TEO + Cz	97.1 ± 4.2[a]	24.5 ± 14.4[cd]	0.0 ± 0.0[d]	0.0 ± 0.0[e]

Data are means ± standard deviation of triplicates (*n* = 3). Means in the same column with different letters are significantly different (*p* ≤ 0.05). CS = chitosan; TPP = Tripolyphosphate; CEO = Cinnamon EO; TEO = Thymus EO; and Cz = Czapek.

non-septate hyphae (coenocytic) at 12 h of incubation of *A. parasiticus*, both in the control and in the treatments. A higher percentage of non-septate hyphae was found in the Czapek control (C_{CZ}) and in the treatment with CS-CEO nanoparticles (31.5 and 33.3%, respectively). In the CS-TEO nanoparticles, 27.8% of the hyphae had two septate. No effect of the CS-EO nanoparticles was observed in the formation of septate in the hyphae, probably because of interactions that could have occurred among the EO, chitosan, and Tween 80 (Cota-Arriola *et al.,* 2013).

Anti-aflatoxigenic assay

The production of total aflatoxins in maize grains was not inhibited. No significant difference was found among the treatments, only with respect to maize grain controls without the fungus (1.0 ± 0.7). Contrary to our expectations, EO encapsulated in chitosan particles showed no anti-aflatoxigenic effect, and no individual effects of the EO or chitosan was observed, indicating that they were not capable of suppressing the production of AFB_1. The AFB_1 production in ppb was 1,233.3 in chitosan, 1,433.3 in TPP, and from 1,200 – 1,300 in the others. This finding is not in agreement with some studies on the *Aspergillus* species, which evaluated chitosan encapsulated EO and that these reduced AFB production. Yavad *et al.* (2019) reported that *Myristica fragrans* Houtt. EO encapsulated in chitosan completely inhibited growth and AFB_1 production of *A. flavus*. They mentioned that this could be due to the loss of volatile compounds and possible negative interaction with the composition of the growth media. Furthermore, Kumar *et al.* (2019) nano-encapsulated a mixture of thymol, methyl cinnamate, and linalool in chitosan that completely inhibited the growth and AFB_1 production by *A. flavus*. They speculated that the antifungal mode of action was related to the decrease in ergosterol content, membrane ion leakage, impairment in carbon-source utilisation, mitochondrial functioning, the anti-oxidative defence system (SOD, CAT, and GR), and Ver-1 gene of AFB_1 biosynthesis. Also, López-Meneses e*t al.* (2018) evaluated chitosan nanoparticles with *Schinus molle* EO in the production of aflatoxins, reporting an inhibitory effect at 250 and at 500 ppm. Moreover, Sinha *et al.* (1993) found a significant reduction (78%) in aflatoxin production in liquid media after treatment with more than 100 μg/mL of cinnamon EO. On the other hand, Dwivedy *et al.* (2018) found that the production of AFB_1 in pistachios by *A. flavus* was highly reduced when *Illicium verum* EO was nano-encapsulated in chitosan than in

EO alone. It is noteworthy that the concentration of chitosan used was higher (1.5%) than that reported in the present work (0.2%). These variations in the formulation of nanomaterials directly impacted the biological activity that they may present, due to the possible interactions that may arise between the compounds used and the availability of the functional groups responsible for their bioactivity.

Conclusion

The characterisation of EO encapsulated in chitosan indicated that the inclusion of EO in chitosan matrices affects the shape and size of these. Also, FT-IR and EE suggest that the EO could have adhered to the surface of the CS matrices, as observed in the regions of aromatic CH and OH bonds present in the major active phenolic groups of both EO in their respective bands. The antifungal evaluation revealed that CS-CEO and CS-TEO nanoparticles exerted an inhibitory effect on the radial growth and spore germination of *A. parasiticus* in the first hours of incubation, being more susceptible on spores.

On the other hand, there was no significant effect of CS-CEO and CS-TEO nanoparticles on the production of total aflatoxins, as well as on the number of septate in the hyphae of *A. parasiticus*. The results obtained in the present work suggest that it is necessary to continue research in the formulation of this type of materials with antimicrobial potential.

Acknowledgement

References

Alavi, M. and Karimi, N. 2019. Biosynthesis of Ag and Cu NPs by secondary metabolites of usnic acid and thymol with biological macromolecules aggregation and antibacterial activities against multi drug resistant (MDR) bacteria. International Journal of Biological Macromolecules 128: 893-901.

Alavi, M. and Nokhodchi, A. 2020. An overview on antimicrobial and wound healing properties of ZnO nanobiofilms, hydrogels, and bionanocomposites based on cellulose, chitosan, and alginate polymers. Carbohydrate Polymers 227: article ID 115349.

Alavi, M. and Rai, M. 2019. Recent progress in nano-formulations of silver nanoparticles with cellulose, chitosan, and alginic acid biopolymers for antibacterial applications. Applied Microbiology and Biotechnology 103(21-22): 8669-8676.

Cota-Arriola, O., Cortez-Rocha, M. O., Ezquerra-Brauer, J. M., Lizardi-Mendoza, J., Burgos-Hernández, A., Robles-Sánchez, R. M. and Plascencia-Jatomea, M. 2013. Ultrastructural, morphological, and antifungal properties of micro and nanoparticles of chitosan crosslinked with sodium tripolyphosphate. Journal of Polymers and the Environment 21(4): 971-980.

Dananjaya, S. H. S., Erandani, W. K. C. U., Kim, C. H., Nikapitiya, C., Lee, J. and De Zoysa, M. 2017. Comparative study on antifungal activities of chitosan nanoparticles and chitosan silver nano composites against *Fusarium oxysporum* species complex. International Journal of Biological Macromolecules 105(Part 1): 478-488.

Degola, F., Morcia, C., Bisceglie, F., Mussi, F., Tumino, G., Ghizzoni, R., ... and Lodi, T. 2015. *In vitro* evaluation of the activity of thiosemicarbazone derivatives against mycotoxigenic fungi affecting cereals. International Journal of Food Microbiology 200: 104-111.

Dwivedy, A. K., Singh, V. K., Prakash, B. and Dubey, N. K. 2018. Nanoencapsulated *Illicium verum* Hook.f. essential oil as an effective novel plant-based preservative against aflatoxin B_1 production and free radical generation. Food and Chemical Toxicology 111: 102-113.

Elaissi, A., Medini, H., Larbi Khouja, M., Simmonds, M., Lynene, F., Farhat, F., ... and Harzallah-Skhiri, F. 2010. Variation in volatile leaf oils of eleven *Eucalyptus* species harvested from korbous arboreta (Tunisia). Chemistry and Biodiversity 7(7): 1841-1854.

Feyzioglu, G. C. and Tornuk, F. 2016. Development of chitosan nanoparticles loaded with summer savory (*Satureja hortensis* L.) essential oil for antimicrobial and antioxidant delivery applications. LWT 70: 104-110.

Goy, C. R., Morais, S. T. B. and Assis, O. B. G. 2016. Evaluation of the antimicrobial activity of chitosan and its quaternized derivative on *E. coli* and *S. aureus* growth. Revista Brasileira de Farmacognosia 26(1): 122-127.

Hosseini, S. F., Zandi, M., Rezaei, M. and Farahmandghavi, F. 2013. Two-step method for encapsulation of oregano essential oil in chitosan nanoparticles: preparation, characterization and *in vitro* release study. Carbohydrate Polymers 95(1): 50-56.

Jemaa, M. B., Falleh, H., Serairi, R., Neves, M. A., Snoussi, M., Isoda, H., ... and Ksouri, R. 2018. Nanoencapsulated *Thymus capitatus* essential oil as natural preservative. Innovative Food Science and Emerging Technologies 45: 92-97.

Juglal, S., Govinden, R. and Odhav, B. 2002. Spice oils for the control of co-occurring mycotoxin-producing fungi. Journal of Food Protection 65(4): 683-687.

Kalagatur, N. K., Ghosh, O. S. N., Sundararaj, N. and Mudili, V. 2018. Antifungal activity of chitosan nanoparticles encapsulated with *Cymbopogon martinii* essential oil on plant pathogenic fungi *Fusarium graminearum*. Frontiers in Pharmacology 9: article ID 610.

Keawchaoon, L. and Yoksan, R. 2011. Preparation, characterization and *in vitro* release study of carvacrol-loaded chitosan nanoparticles. Colloids and Surfaces B: Biointerfaces 84(1): 163-171.

Kocevski, D., Du, M., Kan, J., Jing, C., Lačanin, I. and Pavlović, H. 2013. Antifungal effect of *Allium tuberosum*, *Cinnamomum cassia*, and *Pogostemon cablin* essential oils and their components against population of *Aspergillus* species. Journal of Food Science 78(5): M731-M737.

Kumar, A., Kujur, A., Singh, P. P. and Prakash, B. 2019. Nanoencapsulated plant-based bioactive formulation against food-borne molds and aflatoxin B_1 contamination: preparation, characterization and stability evaluation in the food system. Food Chemistry 287: 139-150.

Lambert, R. J., Skandamis, P. N., Coote, P. J. and Nychas, G. J. 2001. A study of the minimum inhibitory concentration and mode of action of oregano essential oil, thymol and carvacrol. Journal of Applied Microbiology 91(3): 453-462.

Liu, Q., Meng, X., Li, Y., Zhao, C. N., Tang, G. Y. and Li, H. B. 2017. Antibacterial and antifungal activities of spices. International Journal of Molecular Sciences 18(6): article ID 1283.

López-Meneses, A. K., Plascencia-Jatomea, M., Lizardi-Mendoza, J., Fernández-Quiroz, D., Rodríguez-Félix, F., Mouriño-Pérez, R. R. and Cortez-Rocha, M. O. 2018. *Schinus molle* L. essential oil-loaded chitosan nanoparticles: preparation, characterization, antifungal and anti-aflatoxigenic properties. LWT 96: 597-603.

Luque-Alcaraz, A. G., Cortez-Rocha, M. O., Velázquez-Contreras, C. A., Acosta-Silva, A. L., Santacruz-Ortega, H. C., Burgos-Hernández, A., ... and Plascencia-Jatomea, M. 2016. Enhanced antifungal effect of chitosan/pepper tree

(*Schinus molle*) essential oil bionanocomposites on the viability of *Aspergillus parasiticus* spores. Journal of Nanomaterials 2016: article ID 6060137.

Mohammadi, A., Hashemi, M. and Hosseini, S. M. 2015. Chitosan nanoparticles loaded with *Cinnamomum zeylanicum* essential oil enhance the shelf life of cucumber during cold storage. Postharvest Biology and Technology 110: 203-213.

Mouriño-Pérez, R. R. 2013. Septum development in filamentous ascomycetes. Fungal Biology Reviews 27(1): 1-9.

Mubarak, E. E., Ali, L. Z., Ahmed, I. F. A., Ahmed, A. B. A. and Taha, R. M. 2015. Essential oil compositions and cytotoxicity from various organs of *Eucalyptus camaldulensis*. International al Journal of Agriculture and Biology 17(2): 320-326.

Nabavi, S. F., Di Lorenzo, A., Izadi, M., Sobarzo-Sánchez, E., Daglia, M. and Navabi, S M. 2015. Antibacterial effects of cinnamon: from farm to food, cosmetic and pharmaceutical industries. Nutrients 7(9): 7729-7748.

Pillai, P. and Ramaswamy, K. 2012. Effect of naturally occurring antimicrobials and chemical preservatives on the growth of *Aspergillus parasiticus*. Journal of Food Science and Technology 49(2): 228-233.

Prakash, B., Kujur, A., Yadav, A., Kumar, A., Singh, P. P. and Dubey, N. K. 2018. Nanoencapsulation: an efficient technology to boost the antimicrobial potential of plant essential oils in food system. Food Control 89: 1-11.

Rodríguez, M. S., Albertengo, L., Debbaudt, A. and Agulló, E. 2005. Uso del quitosano en alimentos. In González, A. G. A., Gardea, A. A. and Cuamea, N. F. (eds). Nuevas Tecnologías de Conservación de Productos Frescos Cortados (1st ed). Mexico: Logprint Digital.

Romanazzi, G., Feliziani, E., Baños, S. B. and Sivakumar, D. 2017. Shelf life extension of fresh fruit and vegetables by chitosan treatment. Critical Reviews in Food Science and Nutrition 57(3): 579-601.

Russo, M., Serra, D., Suraci, F. and Postorino, S. 2012. Effectiveness of electronic nose systems to detect bergamot (*Citrus bergamia* Risso et Poiteau) essential oil quality and genuineness. Journal of Essential Oil Research 24(2): 137-151.

Said, Z. B. O. S., Haddadi-Guemghar, H., Boulekbache-Makhlouf, L., Rigou, P., Remini, H., Adjaoud, A., ... and Madani, K. 2016. Essential

oils composition, antibacterial and antioxidant activities of hydrodistillated extract of *Eucalyptus globulus* fruits. Industrial Crops and Products 89: 167-175.

Sinha, K. K., Sinha, A. K. and Prasad, G. 1993. The effect of clove and cinnamon oils on growth of and aflatoxin production by *Aspergillus flavus*. Letters in Applied Microbiology 16(3): 114-117.

Soliman, E. A., El-Moghazy, A. Y., El-Din, M. S. M. and Massoud, M. A. 2013. Microencapsulation of essential oils within alginate: formulation and *in vitro* evaluation of antifungal activity. Journal of Encapsulation and Adsorption Sciences 3: 48-55.

Sotelo-Boyás, M. E., Correa-Pacheco, Z. N., Bautista-Baños, S. and Corona-Rangel, M. L. 2017b. Physicochemical characterization of chitosan nanoparticles and nanocapsules incorporated with lime essential oil and their antibacterial activity against food-borne pathogens. LWT 77: 15-20.

Sotelo-Boyás, M., Correa-Pacheco, Z., Bautista-Baños, S. and Gómez-Y-Gómez, Y. 2017a. Release study and inhibitory activity of thyme essential oil-loaded chitosan nanoparticles and nanocapsules against foodborne bacteria. International Journal of Biological Macromolecules 103: 409-414.

Villegas-Rascón, R. E., López-Meneses, A. K., Plascencia-Jatomea, M., Cota-Arriola, O., Moreno-Ibarra, G. M., Castillón-Campaña, L. G., … and Cortez-Rocha, M. O. 2018. Control of mycotoxigenic fungi with microcapsules of essential oils encapsulated in chitosan. Food Science and Technology 38(2): 335-340.

Williams, J. H., Phillips, T. D., Jolly, P. E., Stiles, J. K., Jolly, C. M. and Aggarwal, D. 2004. Human aflatoxicosis in developing countries: a review of toxicology, exposure, potential health consequences, and interventions. The American Journal of Clinical Nutrition 80(5): 1106-1122.

Woranuch, S. and Yoksan, R. 2013. Eugenol-loaded chitosan nanoparticles: I. Thermal stability improvement of eugenol through encapsulation. Carbohydrate Polymers 96(2): 578-585.

Xing, K., Zhu, X., Peng, X. and Qin, S. 2015. Chitosan antimicrobial and eliciting properties for pest control in agriculture: a review. Agronomy for Sustainable Development 35: 569-588.

Yavad, A., Kujur, A., Kumar, A., Singh, P. P., Prakash, B. and Dubey, N. K. 2019. Assessing the preservative efficacy of nanoencapsulated mace essential oil against food borne molds, aflatoxin B[1] contamination, and free radical generation. LWT 108: 429-436.